Nature Environment and Pollution Technology
An International Quarterly Scientific Journal

p-ISSN: 0972-6268
(Print copies up to 2016)
e-ISSN: 2395-3454

Vol. 23 | No. 2 | pp. 947-957 | 2024

Original Research Paper

https://doi.org/10.46488/NEPT.2024.v23i02.029

Open Access Journal

The Stabilization of Copper and Cadmium in The Hydrated CaO-CuO-SiO_2 and CaO-CdO-SiO_2 Composites

A. K. Prodjosantoso*†, Y. Febriadi*, A. R. P. Utami and M. P. Utomo***

*Department of Chemistry, Yogyakarta State University, Depok, Yogyakarta, Indonesia

**Department of Chemistry, Manado State University, Tondano, North Sulawesi, Indonesia

†Corresponding author: A.K. Prodjosantoso; prodjosantoso@uny.ac.id

Nat. Env. & Poll. Tech.
Website: www.neptjournal.com

Received: 05-09-2023
Revised: 26-10-2023
Accepted: 06-11-2023

Key Words:
Stabilization
TCLP
Calcium silicate
Heavy metals
Composites

ABSTRACT

The stabilization of toxic metals in the stable matrices is quite well-known. Research on copper and cadmium stabilization in the CaO-CuO-SiO_2 and CaO-CdO-SiO_2 composites was conducted to study the characteristics of CaO-CuO-SiO_2 and CaO-CdO-SiO_2 composites as well as the Cu and Cd metals stabilization in the hydrated composites. The composites of CaO-CuO-SiO_2 and CaO-CdO-SiO_2 were synthesized by the solid-state reaction method. A stoichiometric amount of CaO, SiO_2, $Cu(NO_3)_2$, and CdO were calcined at 1050°C for 4 hours. The synthesized compounds were further hydrated in a soaking time of 30, 60, and 90 days. The hydration produced calcium silicate hydrate that can stabilize metals. The Cu and Cd stability in CaO-CuO-SiO_2 and CaO-CdO-SiO_2, respectively, were tested using the Toxicity Leaching Procedure (TCLP) method. The hydrated and hydrated composite characterizations were performed using X-ray diffraction (XRD), Fourier Transform Infra-Red Spectrophotometer (FTIR), and Scanning Energy Mocroscopy-Energy Dispersive X-ray analyzer (SEM-EDX) and the Atomic Absorption Spectroscopy (AAS) methods. The composites mainly consist of Ca_3SiO_5, Ca_2SiO_4, $Ca(OH)_2$, SiO_2, and metal oxide of CuO, Cu_2O, and CdO. The composites were able to stabilize ~100% of the heavy metals of Cu and Cd.

INTRODUCTION

Heavy metals can cause environmental pollution. In the environment, gradually heavy metals will be absorbed by and accumulated in living organisms. Bioaccumulation of heavy metals can occur in plants, animals, and humans and cause serious health problems. Some metals that can cause health problems are cadmium (Cd) and copper (Cu) (Hossain et al. 2019).

Copper is toxic to certain levels of the human body. Poisoning of this metal can be acute or through accumulation first. Acute poisoning by Cu causes symptoms such as nausea, vomiting, abdominal pain, hemolysis, nephrosis, seizures, and death. Chronic copper poisoning can occur in the liver, leading to hemolysis (Gaetke et al. 2014).On the other hand, cadmium has negative effects on adult humans, including bone damage, cardiovascular disease, and heart disease. Other effects of cadmium are arthritis, kidney failure, and an increased risk of breast cancer (Chen et al. 2016). Those reasons motivate researchers to stabilize heavy metals to reduce pollution using the stabilization/solidification (S/S) method. The S/S technology is based on stabilizing waste, both physically and chemically. Cement, lime, and dissolved silica are often used in the S/S process so that the metals do not leak into the environment (Singh & Budarayavalasa 2021).

Composites from a mixture of CaO and SiO_2 can be used to stabilize heavy metals. The reaction between the two compounds will produce calcium silicate compounds. CaO compounds can be obtained from chicken and duck eggshells. This is because eggshells contain 94-97% $CaCO_3$. The source of CaO compounds can be chosen from eggshells because of their high abundance and priceless. The oxide of SiO_2 can be obtained from nature. Many plants contain silica compounds. Reeds are one of the plants containing silica. However, the use of reeds as a source of SiO_2 is rare (Al-Jubouri et al. 2021).

Hydration is a reaction between certain compounds and water. The reaction can proceed eventually depending on the reactivity of the cation that is substituted (Prodjosantoso 2010). Calcium silicate reacts with water will form calcium silicate hydrate and calcium hydroxide compounds (Schlegel et al. 2015).

One of the main methods for measuring the leaching of heavy metal from the composite is the use of standard

leaching tests. The most used procedure is the Toxicity Characteristic Leaching Procedure (TCLP) of the United States Environmental Protection Agency (USEPA). The TCLP test is needed to determine the absorption rate of copper and cadmium in CaO-CuO/CdO-SiO_2 composites. This test can determine the degree of stabilization of copper and cadmium.

Over the past five years, more than nine hundred articles and journals on heavy metals have been published. This shows how critical the heavy metal problem is. Efforts to stabilize heavy metals with various breakthroughs need to be made. Research by Prodjosantoso and Kennedy (2003) on heavy metals Mg, Cd, Pb, and Ba in the cement phase $Ca_3Al_2O_6$ states that the change in the cement phase after the inclusion of foreign metals in the structure has a large area for further study with various heavy metals and types of composites.

Based on the description above, the purpose of this study is to determine the amount of metal that is stabilized in composites. This study has a great chance of obtaining the result that heavy metals will not be leached after a certain time of the hydration process.

MATERIALS AND METHODS

Composite Synthesis

The calcium oxide extracted from the powdered eggshell was mixed with the silicon dioxide from the reeds in a crucible. Calcining powder calcium oxide from eggshells and calcining powder silicon dioxide from reed plants were assumed to be pure calcium dioxide (CaO) and pure silicon dioxide (SiO_2). Thus, the molecular mass of these two powders was assumed to be equal to the relative mass of the pure compound. A mixture of these two materials was added with metals ($Cu(NO_3)_2.3H_2O$ and CdO) to form a mixture of 1.8 CaO: 0.2 MO (metal oxide): 1 SiO_2. Then ethanol was added into the mixture and crushed until homogeneous, then dried. Drying was carried out using an oven at 110°C for 4 hours so that a dry mixture was obtained. The dry mixture was calcined at 1050°C for 4 hours and was cooled at room temperature to obtain the CaO-MO-SiO_2 composite. The samples were characterized using XRD, FTIR, and SEM-EDX methods.

Composite Hydration

A total of 5 grams of the composite was soaked in 500 mL of water for 30, 60, and 90 days. After soaking, this mixture was filtered off using a 600 mesh sieve to separate the filtrate from the precipitate. The precipitate was dried using an oven at 105°C for 1 h so that a dry hydrate composite was obtained. The filtrate was evaluated using AAS to determine the rest of the metal that had not been entangled in the composite. Dry hydrate composites were characterized using FTIR.

Extractor Solution Determination

A total of 0.5 g of dry hydrate composite was put into a 250 mL beaker, added with 9.65 mL of water, and stirred using a magnetic stirrer for 5 min. The homogeneous composite mixture was then filtered off to obtain the filtrate. The pH of the filtrate was measured to determine the type of extractor solution. According to Kumar et al. (2016), two types of extractor solutions can be used. When the pH of the filtrate is < 5, extractor solution #1 of 5.7 mL of glacial acetic acid (98%) and 64.3 mL NaOH 1 N can be used. When the pH is more than 5, extractor solution #2 of 5.7 mL of glacial acetic acid can be nominated. All samples indicated a pH of > 5.

TCLP (Toxicity Characteristic Leaching Procedure)

Two grams of dry hydrated composite was added into a 250 mL Erlenmeyer, and then 40 mL of extractor #2 solution was added and stirred in an incubator for 18 hours at a rate of 60 rpm. The homogeneous mixture was then filtered off using filter paper to separate the filtrate (liquid phase) from the precipitate (solid phase). The liquid phase was characterized using the AAS method to determine the concentration of metal leached from the TCLP process. In contrast, the solid phase was characterized using XRD, FTIR, and SEM methods.

RESULTS AND DISCUSSION

The composite of CaO-CuO-SiO_2 and CaO-CdO-SiO_2 was successfully synthesized (Table 1.). The composites were characterized using the XRD Rigaku MiniFlex 600 operating Cu-Kα radiation (1.541874 Å) at 2θ° angle from 2° to 80°.

Table 1: Sample code.

Treatment	Code	
	CaO-CuO-SiO_2	CaO-CdO-SiO_2
Composite	Cu.h0	Cd.h0
30-day hydrated composite	Cu.h30	Cd.h30
60-day hydrated composite	Cu.h60	Cd.h60
60-day hydrated composite	Cu.h90	Cd.h90
30-day hydrated composite and TCLP	Cu.h0T	Cd.h30T
60-day hydrated composite and TCLP	Cu.h30T	Cd.h60T
90-day hydrated composite and TCLP	Cu.h90T	Cd.h90T

The XRD diffractogram of unhydrated CaO-CuO-SiO_2 composite (Cu.h0) is described in Fig. 1., indicating that the calcined mixture of eggshell and reeds consists of calcium silicates (Ca_3SiO_5 (30.1%) and Ca_2SiO_4 (59.2%)), calcium hydroxide ($Ca(OH)_2$ (8.0%)), cristobalite (SiO_2 (2.2%)), copper tenorite (CuO (0.3%)), and unidentified species. Tricalcium silicate (Ca_3SiO_5) is characterized by lines at 2θ° angles of 18.30°; 23.42°; 29.76°; 31.40°; 32.56°; 34.62°; 35.90°; 39.16°; 41.54°; and 43.44°, which are in agreement with COD No. 1540705 data. This is also in accordance with Chen et al. (2007) finding that the XRD diffractogram of Ca_3SiO_5 is at 2θ° around 23°, 29°, and 31°.

The compound Ca_2SiO_4 is indicated by XRD lines at 2θ° = 23.42°; 29.76°; 32.56°; 34.62°; 41.54°; 43.44°; 44.93°; 46.04°; 47.80°; 48.80°; 51.16°; 53.90°; 56.74°; 58.65°; 60.87°; and 68.52°. These peaks are in accordance with the results of the research of Mei et al. (2020) and COD No. 1546025. The phase of $Ca(OH)_2$ is indicated by lines at 2θ° about 51.16° ,°18.30, and 56.74°, which is in accordance with COD No. 1000045. Samanta et al. (2016) state that $Ca(OH)_2$ (calcite) is indicated by a line at 2θ° around 51°.

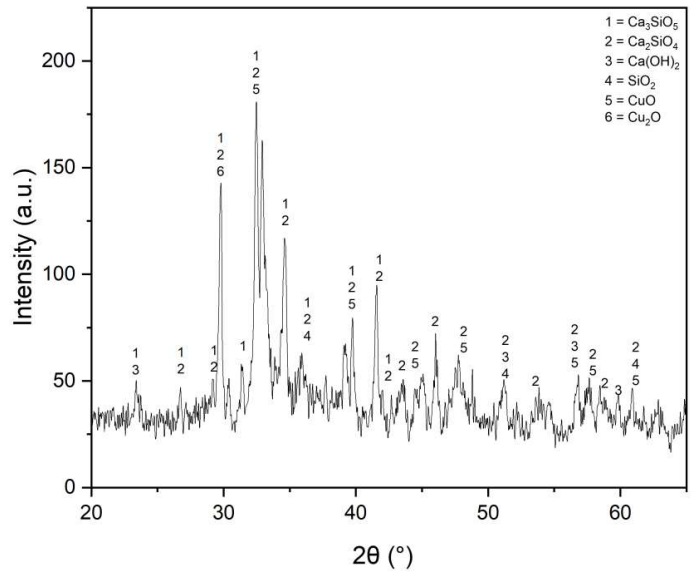

Fig. 1: The XRD diffractogram of Cu.h0 composite.

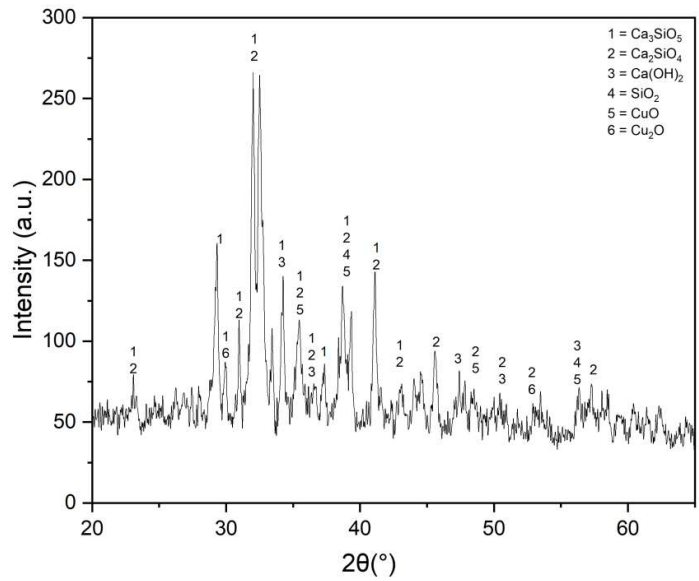

Fig. 2: The XRD diffractogram of Cu.h90T composite.

The compound of SiO_2 is indicated by peaks at 2θ° of 35.90°, 51.16°, and 68.52°. The peaks at 51.16° and 68.52° are in agreement with Geng et al. (2023) for α-SiO_2. Copper compounds of CuO and Cu_2O are observed. The CuO occurs typically at 2θ° angles of 32.48°, 46.04°, 39.16°, 51.16°, 58.65°, and 68.52°, which are in accordance with COD No. 1526990, and Filiz (2020). The Cu_2O cuprite is indicated by the presence of peaks at 2θ° = 29.76 °, which is in accordance with COD No. 1000063 data (Animasahun et al. 2021).

The Cu.h90T composite is the hydrated sample for 90 days. The XRD diffractogram indicates 2θ° lines at 23.08°; 29.30°; 29.95°; 30.98°; 32.00°; 34.22°; 35.44°; 36.62°; 37.32°; 38.70°; 41.10°; and 43.04° (Fig. 2) for Ca_3SiO_5 (COD data No. 1540705). Chen et al. (2007) confirmed that the XRD diffraction peaks of the Ca3SiO5 compound are at 2θ° = 23° and 29°. Another silicate, Ca2SiO4 compound, is identified by diffraction peaks at 2θ° = 23.08°; 30.98°; 32.00°; 35.44°; 36.62°; 38.70°; 41.10°; 43.04°; 45.60°; 48.40°; 50.92°; 52.97°; 56.34°; and 57.28° which is in agreement with COD No. 1546025. 2θ°, and the findings of Mei et al. (2020).

XRD lines at *2θ°* = 34.22°; 36,62°; 47,40°; 50,92°; and 56.34° indicate the presence of $Ca(OH)_2$ compound (Samanta et al. 2016, COD data No. 1000045). The lines at 2θ° around 38.70° and 56.34° indicate the existence of the SiO_2 compound. The lines at 2θ° = 29.95 ° and 52.97° indicate the presence of Cu_2O (COD No. 1000063), while the lines at 35.44°, 38.70°, and 48.40° indicate a typical line of CuO (COD No. 1526990, Filiz, 2020). Analyzing using Match! 3 indicates the presence of Ca_3SiO_5 (20.4%), Ca_2SiO_4 (61.5%), $Ca(OH)_2$ (4.7%), SiO_2 (5.6%), CuO (7.7%), Cu_2O (0.1%), and an unidentified species (13.5%).

Based on the XRD diffractograms, Cu.h0T and Cu.h90T samples are crystalline phases. In addition, the samples contain Ca_3SiO_5, Ca_2SiO_4, $Ca(OH)_2$, SiO_2, CuO, and Cu_2O specieses.

The XRD diffractogram of the Cd.h0 is shown in Fig. 3. The XRD diffractogram of the Cd.h0 sample consisting of several lines indicating the presence of CdO (cadmium oxide monteponite), SiO_2 (cristobalite), Ca_3SiO_5 (alite), Ca_2SiO_4 (silicate), and $Ca(OH)_2$.

Based on analysis using Match 3, the percentage of compounds Ca_3SiO_5 is 18.6%; Ca_2SiO_4 27.4%; $Ca(OH)_2$ 40.2 %; SiO_2 13.3%; and CdO 0.2%. The percentage of metal Cd is observed to be very small. This is because Cd evaporated when subjected to heating during the sample treatment (Prodjosantoso & Kennedy 2003).

The diffraction lines at 2θ° = 32.85° and 54.80° indicate the CdO. This is in accordance with the finding of Munawar et al. (2020), showing the XRD lines at 2θ° = 32° and 55°. The SiO2 XRD lines are observed 2θ° = 36.10°; 39.58°; 41.47°; 54.80°; 63.18°; and 64.78°. Typical lines appearing at 2θ° = 21.95°; 23.25°; 29.56°; 32.85°; 34.47°; 36.10°; 39.58°; 41.47°; 43.29°; 45.91°; 47.58°; 51.25°; 53.48°; 54.80°; 59.85°; and 63.18° indicate the presence of Ca2SiO4 which is in agreement with COD No. 1546025. Lines at 2θ° = 18.25°; 21.95°; 23.25°; 29.56°; 32.85°; 34.47°; 36.10°;

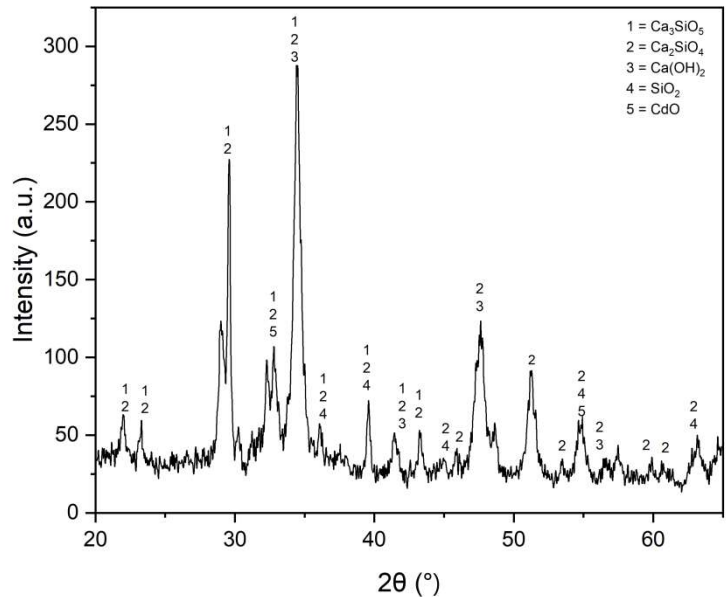

Fig. 3: The XRD diffractogram Cd.h0 sample.

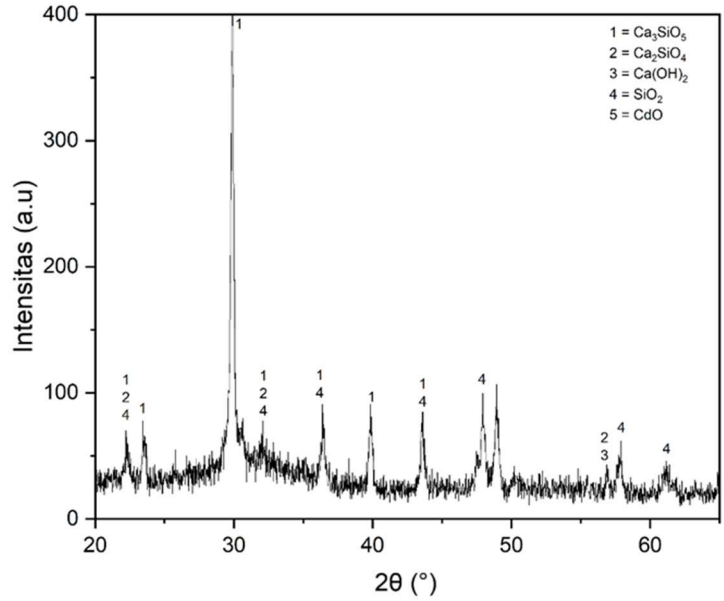

Fig. 4: The XRD diffractogram sample Cd.h90T composite CaO-CdO x-SiO_2 after 90 days of hydration and TCLP.

39.58°; 41.47°; and 43.29° indicate the presence of Ca3SiO5 (COD No. 1540705). Chen et al. (2007) state that the XRD lines of Ca3SiO5 are about 2θ°= 23° and 29°. The lines at 2θ° - 18.25°; 34.47°, 47.58°, and 56.59° indicate the Ca(OH)2 (COD No. 1000045, Samanta et al. 2016).

The XRD diffractogram of Cd.h90T is depicted in Fig. 4. Analysis of the XRD diffractogram of Cd.h90T using Match! 3 indicate the percentage of Ca_3SiO_5 of 58.7%; Ca_2SiO_4 21.8 %; $Ca(OH)_2$ 1.0%; SiO_2 18.3%; CdO 0.1%, and some unidentified peak 17.7%.

The XRD diffraction peaks at 2θ° = 22.28°; 23.53°; 29.89°; 32.00°; 36.41°; 39.86°; and 43.58° indicate the presence of Ca_3SiO_5 (COD No. 1540705, Chen et al. 2007). The peaks at 2θ° = 18.63°; 22.28°; 32.00°; 56.90°; 65.02°; and 70.66° indicate the presence of Ca_2SiO_4. The line at 2θ° 56.90° indicates the presence of $Ca(OH)_2$ (COD No. 1000045). The lines are also observed at 2θ° = 22.28°; 32.00°; 36.41°; 43.58°; 47.94°; 61.18°; 66.10°; and 70.66° indicating the SiO_2 and at 2θ° = 66° indicating the presence of CdO (Munawar et al. 2020).

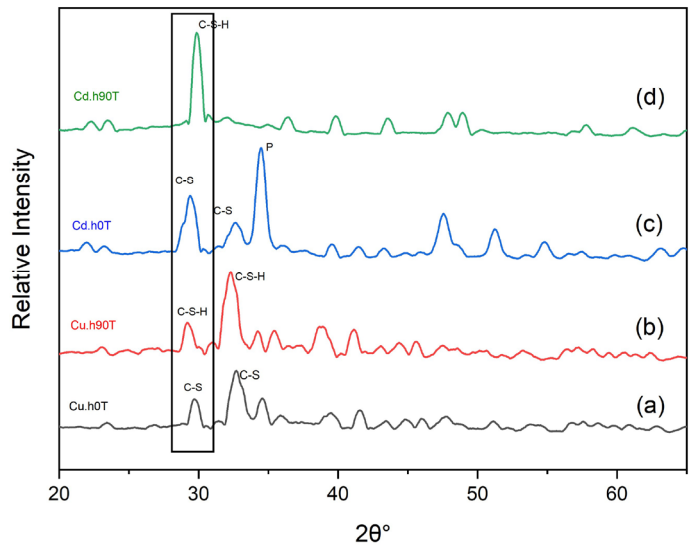

Fig. 5: The XRD diffractogram of (a) Cu.h0, (b) Cu.h90T, (c) Cd.h0, and (d) Cd.h90T samples.

Table 2: The FTIR absorption data of CaO-CuO-SiO_2

Interpretation	Wavenumber [cm^{-1}]		
	Cu.h0	Cu.h90	Cu.h90T
O-H streching of $Ca(OH)_2$	3625	3627	3595
O-H streching of H_2O	3378	3426	3368
C=O streching of CO_2	2359	2360	2357
C-O streching of CaCO3	1405 1435 1477	1414	1419
Streching asymmetri Si-O of C-S-H	985	967	996
Ca-O streching	869	871	872
Si-O-Si group	672	669	668
streching O-Si-O of SiO_2	500	495	492

The XRD diffractogram of composite undergoes a shift after the hydration process and TCLP test (Fig. 5). According to Maddalena et al. (2019) the shifts from $2\theta° = 29.76°$ to 29.30° and from 29.56° to 29.89° for CaO-CuO-SiO_2 and CaO-CdO_x-SiO_2, respectively, indicate the formation of calcium silicate hydrate (C-S-H).

The shifts of the XRD diffractogram are due to the formation of new phases, namely CaO-CuO-SiO_2 and CaO-CdO-SiO_2. In the new phases, the Ca^{2+} ions are partly replaced by copper and cadmium ions in the Cu.h90T and Cd.h90T, respectively. The diameters of the Ca^{2+}, Cu^{+}, $Cu^{2+,}$ and Cd^{2+} ions are 114 pm, 91 pm, 87 pm, and 97 pm, respectively. Thus, due to the ions substituting Ca^{2+} are smaller, the XRD lines are shifted to the right (Fig. 5).

Samples obtained by calcining a mixture of eggshell, reed ash, and metal oxide were analyzed using FTIR to identify the existence of the functional groups of the compounds in the sample. The vibrations of the samples are listed in Table 2.

The FTIR spectra of Cu.h0, Cu.h90, and Cu.h90T samples are similar (Fig. 6.). The difference is noticeable in the intensity of the peaks spectra, indicating the difference in the quantitative amount of components in the samples.

The O-H vibration at 3200-3600 cm^{-1} is stronger, along with hydration treatment and TCLP on the samples. The increase in O-H spectra is due to the hydration of CaO-producing $Ca(OH)_2$. The presence of Ca-O in the $Ca(OH)_2$ is indicated by absorption at a wavenumber of 800 cm^{-1}. The $Ca(OH)_2$ readily reacts with CO_2 from air through the following reaction.

$$CaO + H_2O \rightarrow Ca(OH)_2$$

$Ca(OH)_2 + CO_2 \rightarrow CaCO_3$ (Prodjosantoso et al. 2021).

The formation of $CaCO_3$ is supported by the presence of a peak indicating the C-O stretching in the $CaCO_3$. This peak is weak in the unhydrated sample and is stronger in hydrated and TCLP samples, indicating the increase of $CaCO_3$ in the unhydrated sample. The increase of $CaCO_3$ is due to the carbonation of CaO and/or $Ca(OH)_2$. According to Imani et al. (2022), hydrated CaO reacts with CO_2, producing $CaCO_3$. The CO_2 in the sample is indicated by the absorption at 2400 cm^{-1} (Bekhti et al. 2021).

The peak at 900 cm^{-1} indicates the presence of a Ca-Si-O bond. Hydration treatment causes the absorption of Ca-Si-O to increase in intensity. This is due to the increased amount of C-S-H bonds caused by hydration. The increase in C-S-H is also supported by the presence of free water (H_2O), which is indicated by weak absorption at 3400 cm^{-1} (Saidani et al., 2018).

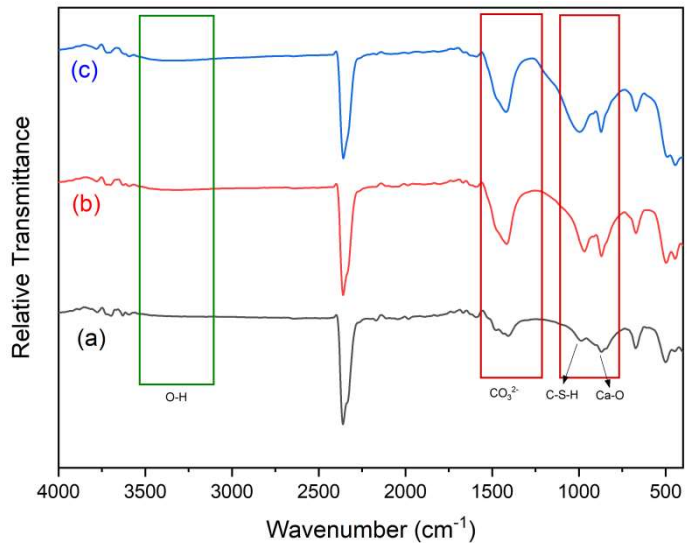

Fig. 6: The FTIR spectra of (a) Cu.h0, (b) Cu.h90, and (c) Cu.h90T.

Table 3: $CaO-CdO_x-SiO_2$ composite FTIR data absorption.

Interpretation	Wavenumber [cm^{-1}]		
	Sample Cd.h0	Sample Cd.h90	Sample Cd.h90T
O-H *streching* of H_2O	3632	3592	3429
O-H *streching* of $Ca(OH)_2$	3375	3395	3375
C=O *streching* of CO_2	2359	2358	2357 2332
C-O *streching* of $CaCO_3$	1408	1408	1413
Ca-O-Si	997	966	962
Ca-O *streching*	910 873	873	870
Si-O-Si group	706 669	706 666	702 660
O-Si-O *streching* of SiO_2	500	445	443

The FTIR spectra of $CaO-CdO-SiO_2$ are comprised of various absorption peaks (Table 3).

The FTIR spectra of hydrated and unhydrated samples are depicted in Fig. 7. The FTIR spectra differences between Cd.h0 with Cd.h90 and Cd.h90T are observed. The spectra of the hydrated sample observed at 3200-3600 cm^{-1} are stronger than the unhydrated. This is due to the reaction of CaO with water, forming $Ca(OH)_2$.

In the C-O absorption area, the asymmetry of $CaCO_3$ absorption peaks is stronger. This indicates that there is an increase in $CaCO_3$ after hydration, according to research from Bekhti et al. (2021). Conversely, the Ca-O absorption area at 910-870 cm-1 experienced attenuation of absorption. This is because Ca in CaO is replaced by Cd metal, and then Ca in Ca-Si-O bonds increases in the wavenumber range 1050-

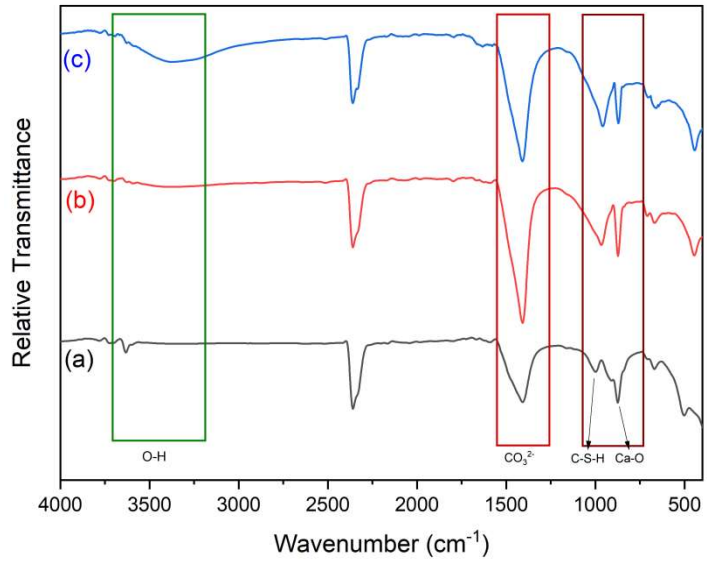

Fig. 7: The FTIR spectra of (a) Cd.h0), (b) Cd.h90, and (c) Cd.h90T.

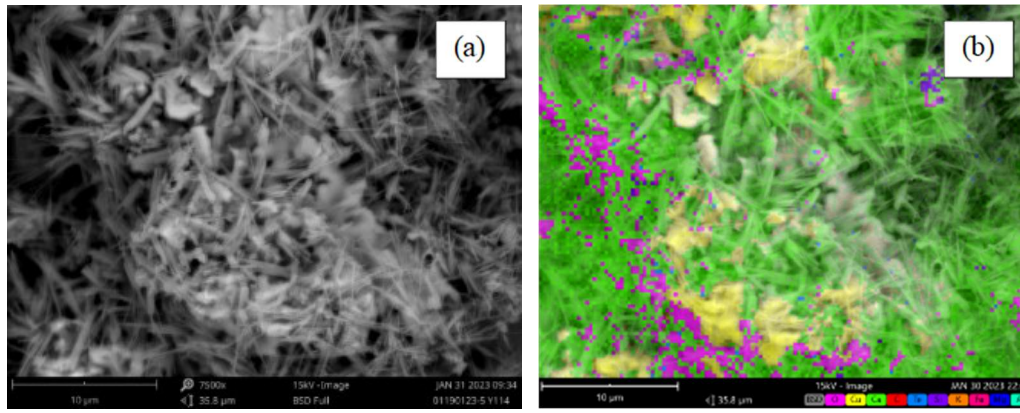

Fig. 8: the surface morphology of Cu.h0 with 7500x magnification (a) and mapping (b).

950 cm^{-1}. This is in accordance with Yang et al. (2022) research.

Selected SEM micrographs of Cu.h0 are presented in Fig. 8. The sample is elongated fibers with a length of about 3 µm. The particles are evenly distributed, and agglomerations are not observed. In addition to observing the surface with SEM, surface analysis was also undertaken using EDX to determine the elements composing the sample (Fig. 8). The distribution of elements is observed to be homogeneous with the dominance of Ca (green). The Cu element is in the middle position, surrounded by other elements.

The EDX analysis of Cu.h0 results in the element composition of the sample (Fig. 9), Ca, Cu, and Si as much as 48.75%; Cu 44.87%; and Si 16.38%, respectively. The tiny amount of other elements detected are K, Fe, Al, and Mg. These elements are in samples as a result of the use of natural material as a precursor. The elements of Al, K, Mg, and Fe were reported to be present in chicken eggshells (Park et al. 2007), and K and Mg are found in reeds (Butler et al. 2021).

The SEM micrographs of Cu.h90T are shown in Fig. 10. The 90-day hydration and TCLP (Fig. 10.) cause the deformation of the particle. The elongated fibers (Fig. 8.) change to rounded particles having about 1 µm in size. The even distribution of Ca and Si is observed (Fig. 10).

The EDX graph (Fig. 11) describes that the percentages of elements Ca, Cu, and Si are (50.63%), (20.84%) and (16.38%), respectively. The percentage of Cu elements decreases after 90 days of hydration and TCLP. In the sample are also observed, unexpected elements such as K, Al, Mg, and P. These elements can be assumed from eggshells and reeds used as precursors.

The SEM was performed on Cd.h0 samples (Fig. 12). The surface of Cd.h0 is irregular in shape. The surface is dominated by the Ca element, which is characterized by the presence of a dominant green color. The Si elements (purple) are slightly visible, while the cadmium elements are not detected.

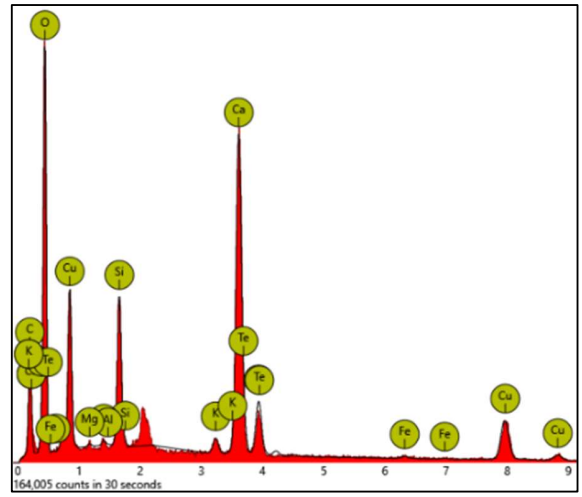

Fig. 9: The EDX of Cu.h0.

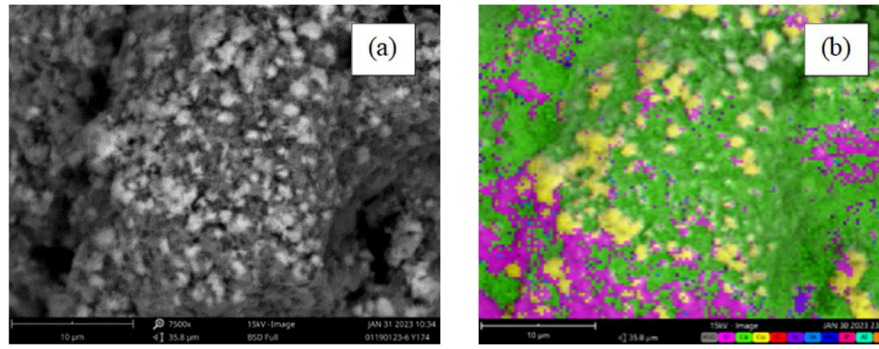

Fig. 10: The SEM micrograph of Cu.h90T.

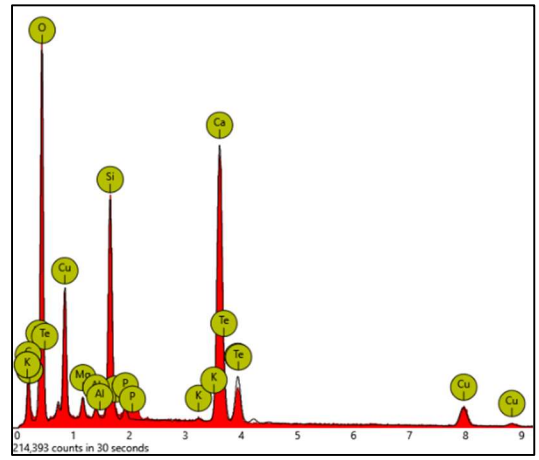

Fig. 11: The EDX graph of Cu.h90T.

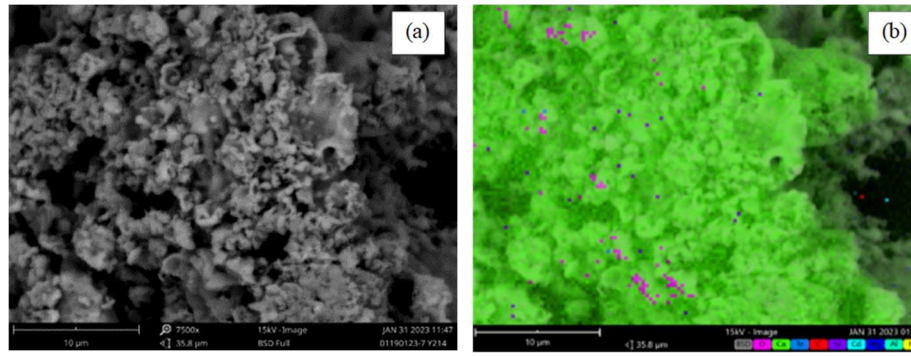

Fig. 12: The surface morphology of Cd.h0.

The SEM micrograph of Cd.h90T can be seen in Fig. 13. The surface of the sample is rough, with no lumps forming. Elemental mapping analysis (Fig. 13. (b)) indicates that the distribution of elements on the sample surface is evenly distributed. The surface is dominated by Ca (green) and the minor of Cd (light blue), which Ca may cover.

The EDX of Cd.h90T (Fig. 14.) shows the percentage of the main constituents of the sample, i.e., Ca (52.9%), Cd (3.44%), and Si (43.66%). There is a decreasing content of Cd metal after the hydration and TCLP samples. It is believed that Cd evaporates during sample preparation (Prodjosantoso & Kennedy 2003).

For tracing the Cu and Cd metals, the hydration and TCLP filtrate of the samples were analyzed using the AAS method.

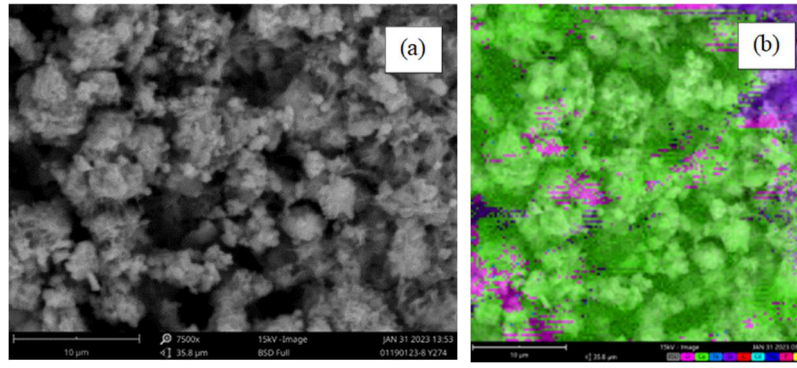

Fig. 13: The surface morphology of Cd.h90T.

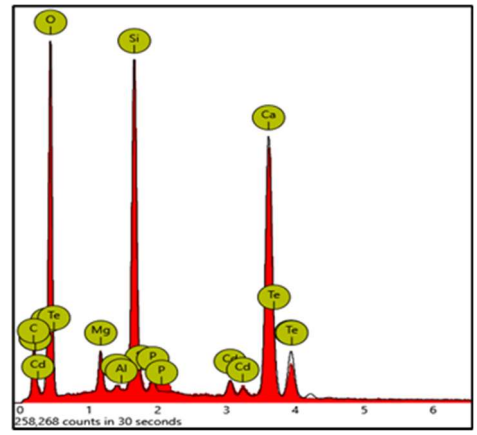

Fig. 14: The EDX of Cd.h90T.

Table 4: The Cu in the hydrated CaO-CuO-SiO_2

Samples	The Cu leached after hydration [$mg.L^{-1}$]	The Cu leached after hydration [mole]	Stabilized Cu in samples [mole]	Percentage of Cu in samples [%]
Cu.h30	0.0113	8.9×10^{-8}	0.199999911	99.99995554
Cu.h60	0.0082	6.5×10^{-8}	0.199999935	99.99996774
Cu.h90	0.0062	5.8×10^{-8}	0.199999951	99.99997561

Table 5: The Cu in CaO-CuO-SiO_2 after TCLP.

Samples	The Cu leached after hydration [$mg.L^{-1}$]	The Cu leached after hydration [mole]	Stabilized Cu in samples [mole]	Percentage of Cu in samples [%]
Cu.h30T	0.0082	5.2×10^{-9}	0.199999906	99.99999742
Cu.h60T	0.0051	3.2×10^{-9}	0.199999932	99.99999839
Cu.h90T	0.0072	4.5×10^{-9}	0.199999947	99.99999773

Table 6: The Cd in the hydrated CaO-CdO-SiO_2.

Samples	The Cd leached after hydration [$mg.L^{-1}$]	The Cd leached after hydration [mole]	Stabilized Cd in samples [mole]	Percentage of Cd in samples [%]
Cd.h30	0.1261	5.6×10^{-7}	0.199999439	99.99971955
Cd.h60	0.1296	5.7×10^{-7}	0.199999424	99.99971177
Cd.h90	0,1228	5.5×10^{-7}	0,199999454	99.99972689

Table 7: The Cd in CaO-CdO-SiO_2 after TCLP.

Samples	The Cd leached after hydration [$mg.L^{-1}$]	The Cd leached after hydration [mole]	Stabilized Cd in samples [mole]	Percentage of Cd in samples [%)
Cd.h30T	0.1193	4.2×10^{-8}	0.199999397	99.99997877
Cd.h60T	0.1222	4.3×10^{-8}	0.19999938	99.99997826
Cd.h90T	0.1225	4.4×10^{-8}	0.19999941	99.99997820

By doing it, the metals retained in the samples are known.

The AAS analysis of CaO-CuO-SiO_2 samples is presented in Table 4. and Table 5.

The AAS analysis of the samples indicates that both the Cu in the hydrated and TCLP samples are ~100% stabilized. However, the amount of leached metals is observed to be very small and safe for the environment.

The AAS analysis of CaO-CdO-SiO_2 samples is presented in Table 6. and Table 7.

Similar to the Cu samples, the AAS analysis of the samples indicates that both the Cd in the hydrated and TCLP samples are ~100% stabilized. However, the amount

of leached metals is observed to be very small and safe for the environment.

CONCLUSIONS

Based on the research, it can be concluded that the CaO-CuO-SiO_2 and CaO-CdO-SiO_2 are composed of the main compounds: Ca_3SiO_5 (alite), Ca_2SiO_4 (silicate), $Ca(OH)_2$ (portlandite), SiO_2 (cristobalite), and metal oxides of CuO (tenorite) and Cu_2O (cuprite), as well as the CdO (mentoponite) for cadmium. The Cu and Cd are stabilized in CaO-CuO-SiO_2 and CaO-CdO-SiO_2 composites by ~100%.

ACKNOWLEDGMENTS

The author would like to thank the Department of Chemistry Education, Yogyakarta State University.

REFERENCES

Al-Jubouri, S.M., Al-Batty, S.I. and Holmes, S. M. 2021. Using the ash of common water reeds as a silica source for producing high purity ZSM-5 zeolite microspheres. Micropor. Mesopor. Mater., 316: 110953, https://doi.org/10.1016/j.micromeso.2021.110953.

Animasahun, L.O., Taleatu, B.A., Adewinbi, S.A., Bolarinwa, H.S. and Fasasi, A.Y. 2021. Synthesis of SnO_2/CuO/SnO_2 multi-layered structure for photoabsorption: compositional and some interfacial structural studies. J. Niger. Soc. Physic. Sci., 3: 74-81. https://doi.org/10.46481/jnsps.2021.160.

Bekhti, H., Boucheffa, Y., Blal, A.H. and Travert, A. 2021. In situ FTIR investigation of CO_2 adsorption over MgO–Impregnated NaY zeolites. Vib. Spectrosc., 117: 103313. https://doi.org/10.1016/j.vibspec.2021.103313.

Butler, O.M., Lewis, T. and Chen, C. 2021. Do soil chemical changes contribute to the dominance of blady grass (Imperata cylindrical) in surface fire-affected forests? Fire, 23 :(2)4. https://doi.org/10.3390/fire4020023.

Chen, C., Xun, P., Nishijo, M. and He, K. 2016. Cadmium exposure and risk of lung cancer: A meta-analysis of cohort and case-control studies among general and occupational populations. J. Expo. Sci. Environ. Epidemiol., 26: 437-444. https://doi.org/10.1038/jes.2016.6.

Chen, Q.Y., Hills, C.D., Tyrer, M., Slipper, I., Shen, H. G. and Brough, A. 2007. Characterization of products of tricalcium silicate hydration in the presence of heavy metals. J. Hazard. Mater., 3)147): 817-825. https://doi.org/10.1016/j.jhazmat.2007.01.136.

Filiz, B.C. 2020. The role of catalyst support on activity of copper oxide nanoparticles for reduction of 4-nitrophenol, Adv. Powder Technol., 9)31): 3845-3859. https://doi.org/10.1016/j.apt.2020.07.026.

Gaetke, L.M., Chow-Johnson, H.S. and Chow, C.K. 2014. Copper: Toxicological relevance and mechanisms. Arch. Toxicol., 11)88): 1929-1938. https://doi.org/10.1007/s00204-014-1355-y.

Geng, C., Mei, Z., Yao, X., Wang, C., Lu, D. and Chen, W. 2023. Effect of the crystalline state of SiO_2 on the compressive strength of cement paste at HTHP. Constr. Build. Mater., 362: 129787. https://doi.org/10.1016/j.conbuildmat.2022.129787.

Hossain, R., Nekouei, R.K., Mansuri, I. and Sahajwalla, V. 2019. Sustainable recovery of Cu and sn from problematic global waste: exploring value from waste printed circuit boards. ACS Sustain. Chem. Eng., **7**(1): 4567. https://doi.org/10.1021/acssuschemeng.8b04657.

Imani, M., Tahmasebpoor, M., Sánchez-Jiménez, P.E., Valverde, J.M. and Moreno, V. 2022. Improvement in cyclic CO_2 capture performance and fluidization behavior of eggshell-derived $CaCO_3$ particles modified with acetic acid used in a calcium looping process. J. CO_2 Util., 65: 102207. https://doi.org/10.1016/j.jcou.2022.102207.

Kumar, K.S., Gandhimathi, R. and Baskar, K. 2016. Assessment of heavy metals in the leachate of concrete made with e-waste plastic. Adv. Civil. Eng. Mater., 5(1): 256-262. https://doi.org/10.1520/ACEM20160003.

Maddalena, R., Li, K., Chater, P. A., Michalik, S. and Hamilto, A. 2019. Direct synthesis of a solid calcium-silicate-hydrate (C-S-H). Constr. Build. Mater., 223: 565-554. https://doi.org/10.1016/j.conbuildmat.2019.06.024.

Mei, K., Cheng, X., Pu, Y., Ma, Y., Gao, X., Yu, Y., Zhuang, J. and Guo, X. 2020. Evolution of silicate structure during corrosion of tricalcium silicate (C_3S) and dicalcium silicate (C_2S) with hydrogen sulfide (H_2S). Corros. Sci. 163: 108301. https://doi.org/10.1016/j.corsci.2019.108301.

Munawar, T., Yasmeen, S., Hussain, F., Mahmood, K., Hussain, A., Asghar, M. and Iqbal, F. 2020. Synthesis of novel heterostructured ZnO-CdO-CuO nanocomposite: characterization and enhanced sunlight driven photocatalytic activity. Mater. Chem. Phys., 249: 122983. https://doi.org/10.1016/j.matchemphys.2020.122983.

Park, H.J., Jeong, S.W., Yang, J.K., Kim, B.G. and Lee, S.M. 2007. Removal of heavy metals using waste eggshells. J. Enviro. Sci., 19(12): -1436 1441. https://doi.org/10.1016/S1001-0742(07)60234-4.

Prodjosantoso, A.K. and Kennedy, B.J. 2003. Heavy metals in cement phases: on the solubility of Mg, Cd, Pb, and Ba in $Ca_3Al_2O_6$. Cem. Con. Res., 7)33): 1077-1084. https://doi.org/10.1016/S0008-8846(03)00017-6.

Prodjosantoso, A., Widiyati, W., Widyawati, A. and Utomo, M. P. 2021. Cement chemistry: Hydration of $Ca_{2-X}Sr_xSiO_4$ compound. Orient. J. Chem., 3)37): 589. https://doi.org/10.13005/ojc/370310.

Prodjosantoso, A.K. 2010. Inorganic Chemical Engineering. Kanisius, Yogyakarta.

Saidani, S., Smith, A., El Hafiane, Y. and Tahar, L. B. 2018. Re-examination of $\beta \rightarrow \gamma$ transformation of Ca_2SiO_4. J. Eur. Ceram. Soc., 38(14): -4756 4767. https://doi.org/10.1016/j.jeurceramsoc.2018.06.11.

Samanta, A., Chanda, D. K., Das, P. S., Ghosh, J., Mukhopadhyay, A. K. and Dey, A. 2016. Synthesis of nano calcium hydroxide in aqueous medium. J Am. Ceram. Soc., 99(3): 787-795. https://doi.org/10.1111/jace.14023.

Schlegel, M. L., Pointeau, I., Coreau, N. and Reiller, P. 2004. Mechanism of europium retention by calcium silicate hydrates: An EXAFS study. Environ. Sci. Technol., 16)38): 4423-4431. https://doi.org/10.1021/es0498989.

Singh, R. and Budarayavalasa, S. 2021. Solidification and stabilization of hazardous wastes using geopolymers as sustainable binders. J. Mater. Cycles. Waste. Manag., 23: 1699-1725. https://doi.org/10.1007/s10163-021-01245-0.

Yang, F., Pang, F., Xie, J., Wang, W., Wang, W. and Wang, Z. 2022. Leaching and solidification behavior of Cu^{2+}, $Cr^{3+,}$ and Cd^{2+} in the hydration products of calcium sulfoaluminate cement. J. Build. Eng., 46**:** 103696. https://doi.org/10.1016/j.jobe.2021.103696.

ORCID DETAILS OF THE AUTHORS

A. K. Prodjosantoso: https://orcid.org/0000-0001-7603-5857